Behavior of Circular concrete columns reinforced with GFRP bars and spirals under axial and eccentric loading

Mohamed Elchalakani [1], Tarek Aly[2] and Waleed Nawaz [3]
[1]Senior Lecturer, School of Civil, Environmental and Mining Engineering, University of Western Australia
[2]Senior Civil Engineer, Civil Division, Network and infrastructure, Public Transport Authority
[3]PhD student, School of Civil, Environmental and Mining Engineering, University of Western Australia

Abstract: A study of the use of Glass fibre-reinforced polymer (GFRP) reinforcement in concrete has been investigated by testing 13 column specimens with length to diameter ratio of 5.3. A total of 11 specimens were fully reinforced (longitudinal and transverse) with GFRP while the other two Specimens were reinforced by longitudinal GFRP bars and traditional steel spirals. The effect of the number of GFRP longitudinal bars, reducing the pitch of the spirals and load eccentricities have been examined. The study shows that the ductility of GFRP reinforced specimens with sufficient transverse reinforcement have increased up by 15% while its capacities is found to be 12.3% lower than those with steel reinforcement. This demonstrate that increasing the number of longitudinal reinforcing bars together reducing the pitch of the GFRP spirals would increase the ductility and load capacity of the member. In addition, the strains of the longitudinal GFRP bars were measured and found well beyond the ultimate strain capacity of the concrete, demonstrating the significant of the confinement provided by the spirals

Keywords: circular reinforced concrete members; GFRP; spirals; axial loading.

1. Introduction

Glass fibre reinforced polymer (GFRP) is well known as an emerging material that is lightweight, high-strength, non-magnetic, and non-corrosive by nature. Its mechanical and physical properties showed that it satisfied the requirements as concrete reinforcement. It is used as one of the potential solutions to the corrosion problems faced with the traditional steel reinforcement. However, GFRP behaves very differently to steel, which warrants extensive research before being used in civil applications. Most notably, the GFRP does not yield at high stresses, therefore it is more brittle. A few international standards such as ACI440.1R-15 (ACI 2015) and CAN/CSA S806-12 (CAN/CSA 2017) recall for the use of GFRP as concrete reinforcement whilst no Australian standard on GFRP-reinforced concrete is available.

It was reported that the compressive strength of GFRP was reasonably high, which equalled approximately half of the design tensile strength. The elastic modulus in compression was also similar to that in tension. This made the stress-strain behaviour of GFRP a constant linear relationship across tension and compression. When embedded in square concrete columns, it was found that the ultimate compressive strains were approximately half of the ultimate tensile strains (Elchalakani et al. 2018a). It was recommended that a reduction factor of 0.35 to the ultimate tensile capacity should be used as a conservative estimate (Hadhood et al. 2016).

To prevent the premature buckling failure of the longitudinal GFRP bars, adequate restraints is provided by the transverse reinforcement. In the study of GFRP stirrups or spirals, a closer pitch is sought due to their lower stiffness and larger deformations at a given load, compared to steel stirrups. The more closely spaced GFRP hoops and spirals increased the overall stiffness of the transverse reinforcement at a relatively low stress level. There is a lack of research on the specific effect of varying the number of longitudinal bars and the pitch of the spiral on the circular concrete columns. Additionally, the effect of the material of the longitudinal bars was not studied as most of the studies opted for using steel spirals in the steel-reinforced control group instead of keeping the GFRP spirals. This study aims to quantitatively examine the effect of each parameter by testing a total of 13 specimens of circular section reinforced with and without GFRP.

2. Experimental Program

2.1 Design of Specimens

The type of the reinforcing material (GFRP vs traditional steel), the pitch of the spirals, the number of longitudinal bars and the loading conditions (concentric, eccentric or flexural loading) are the main

variables used in the experimental program as shown in Table 1. The loading conditions with "C" and F denote concentric and flexural loadings respectively. The numbers of 25, 50 and 75mm shown in table 1 are the eccentricities used for eccentric loading condition.

Table 1. Experimental set up and Specimen details.

Specimen	Longitudinal bar type type	Number of Longitudinal bars	Stirrups Spacing mm	Loading Condition	Longitudinal reinforcement ratio	transverse reinforcement ratio
G3-120-C	GFRP	3	120	C	0.55%	0.94%
G4-120-C	GFRP	4	120	C	0.73%	0.94%
G5-120-C	GFRP	5	120	C	0.92%	0.94%
S4-40-C	Steel	4	40	C	0.86%	2.75%
G4-40-C	GFRP	4	40	C	0.73%	2.75%
G4-40-25	GFRP	4	40	25	0.73%	2.75%
G4-40-50	GFRP	4	40	50	0.73%	2.75%
G4-40-75	GFRP	4	40	75	0.73%	2.75%
S4-80-C	Steel	4	80	C	0.86%	1.39%
G4-80-C	GFRP	4	80	C	0.73%	1.39%
G4-80-25	GFRP	4	80	25	0.73%	1.39%
G4-80-50	GFRP	4	80	50	0.73%	1.39%
G4-80-75	GFRP	4	80	75	0.73%	1.39%

The designs of the Concrete specimens showing the detailed reinforcement are shown in Figure 1. A total of 13 circular columns with height (H) of 1150mm and diameter (D) of 215mm were prepared from Portland cement concrete OPC with maximum coarse aggregate particle size of 10mm. The ratio of H/D is 5.4, classified as columns in accordance to ACI 318 (ACI 2014) and CAN/CSA S6-06 (CAN/CSA 2006). The slenderness ratios Le/r of the specimens were determined in accordance with AS 3600 using Le/r for an unbraced column, where Le is the effective length of the column and r is the radius of gyration of the column cross-section. This gives a slenderness ratio of Le/r = 21.4, classified as short-unbraced column (Le/r ≤ 22) in accordance to AS 3600. The slenderness ratio Le/r is 14.9 if the free deformation zone of 800mm between the top and bottom steel clamps was considered. The lateral displacements were found to be very small at the peak load, therefore were neglected (Elchalakani et al. 2018a, 2019).

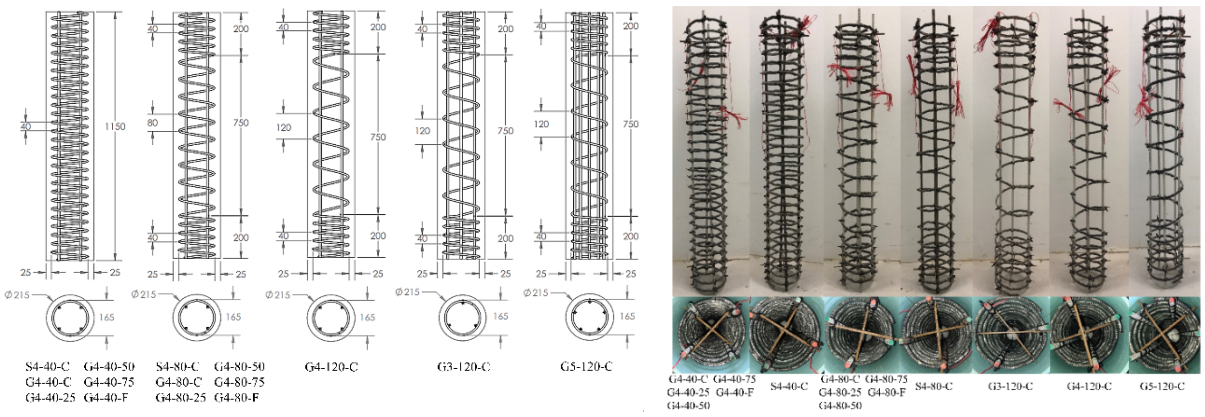

(a) Reinforcement Details of the specimens (dimensions in mm) (b) Reinforcement cages of the specimens

Figure 1. Reinforcement Details.

The pitch of the GFRP spirals were designed to be 40mm throughout the 200mm sections at top and bottom of the columns to eliminate the end effects and shear interactions with the loading platens. Therefore, each column has more than 750mm test region at the center, which corresponds to 65% of the total height of the column specimen. The two ends of the each specimen were prepared so that the longitudinal bars were flushed with the concrete surface and the required total height of was achieved.

2.2 Materials

The specimens were cast using self-compacting concrete SCC with a maximum aggregate size of 10mm and a 28-day characteristic compressive strength of f'c 34 MPa. All workability testing has been undertaken using the slump flow test (AS1012.3.5) and J-ring test (ASTM C1621). In addition, A total of 13 test cylinder specimens (100mm diameter and 200mm height) were cast using the same SCC mix to obtain the compressive strength at 28days of concrete age.

The type of the GFRP and Spirals is known as "MateenBar". This type is manufactured by pulling the glass fibre rovings through and epoxy resin bath then into a heated die to form the required shape. This process is known as pultrusion method to give the GFRP a high tensile strength (Pultron Composites 2016). The longitudinal GFRP bars (10mm nominal diameter) used in this study is characterized by an ultimate tensile strength of $f_{fu,bar}$ = 930 MPa, while the GFRP spirals (8 mm nominal diameter, 165 mm internal diameter) had a reduced ultimate tensile strength of $f_{fu,spiral}$ = 650 MPa (Pultron Composites 2016).

The longitudinal steel bars used in this study were N10 (10mm diameter and normal ductility deformed bars) with a nominal tensile strength of $f_{fu,steel}$ = 500 MPa in accordance to AS/NZS 4671. Table 3 shows the properties of the GFRP and the conventional steel bars. The actual cross sectional areas of the bars were determined using the immersion test method in accordance to ASTMD7205.

The longitudinal steel and GFRP bars (1175mm length) were held in their designed location using a custom made wooden apparatus. Then, the spirals were then stretched across the entire length and attached to the bars using Nylon cable ties so that the correct pitch was achieved. A 30 mm strain gauges were attached to the mid-point of the longitudinal bars to measure the strains developed in the bars. A cover of 25mm across the perimeter of the specimens was achieved using steel spacers attached to the longitudinal bars.

The concrete specimens were cast using PVC formwork with an internal diameter of 215mm and length of 1175mm. Fig 1 shows the reinforcement cages.

2.2 Test Set-up

Figure 2 shows the final set up for testing the reinforced concrete column specimens. All the column specimens were tested at a constant loading rate of 20 kN/min on the 2000 kN Amsler machine using a load control scheme. The measurements of the applied load, vertical displacements from the Amsler machine and the strain gauge readings were recorded until failure of the specimen.

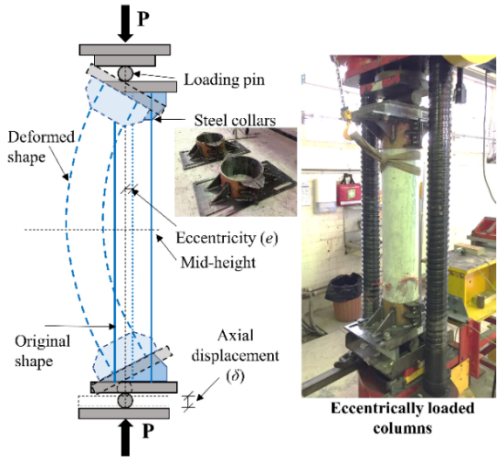

Eccentrically loaded columns

Figure 2. Test setup. **Figure 3. Columns after testing concentrically**

3. Results and Discussions

3.1 Concentrically Loaded Columns

Figure 3 shows the specimens after testing and Figure 4 shows the results of the axial-load deflection curv es for the concentrically loaded columns. The Specimens G4-40-C and S4-40-C with short GFRP spiral pitch (40mm) exhibited highest ductility with the later specimen had 10.8% greater stiffness in the linear elastic range and slightly peak higher peak load. This is attributed to the higher elastic modulus of the conventional steel bares.

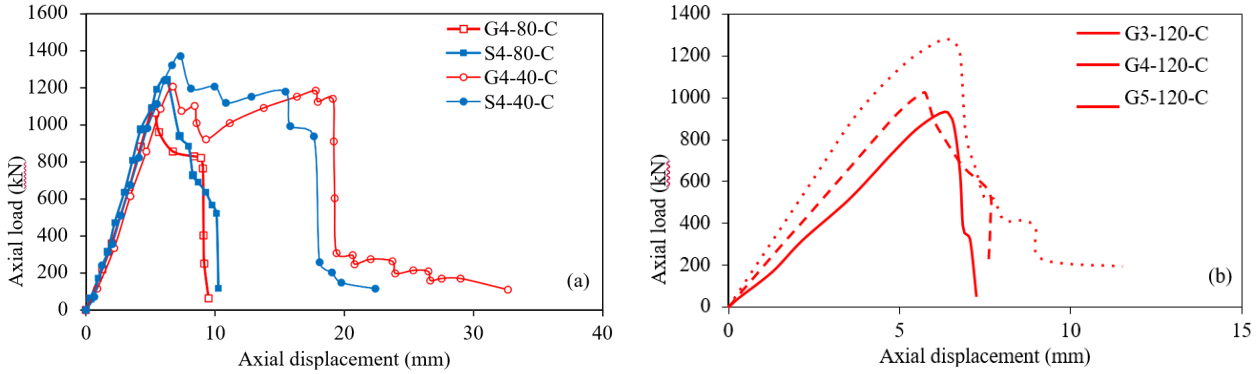

a) steel- and GFRP- reinforced columns with 4 longitudinal bars b) GFRP-reinforced columns with a 120 mm spiral pitch.

Figure 4. Axial load-axial displacement curves for the concentrically loaded columns.

The results show that the first peak load in S4-40-C was 12.5% greater than G4-40-C. This is coincident with the results of 13% difference found by Alsayed et al. (Alsayed et al. 1999). Vertical cracks in the cover started to develop at the mid-height of the specimen, and then spalling in the concrete cover occurred at the peak load, which was followed by a gradual increase in the load to a second peak. This is likely is attributed to the improved strength through the confinement provided by the GFRP spirals. The following peaks were attributed to the failure of the spirals at certain locations.

Figure 5a shows that the strains in the GFRP bar reached approximately εfrp, c = -0.006 whilst strains in the steel bar reached $\varepsilon_{s,c}$ = -0.012. The difference was attributed to the difference in the failure mode of the bars. The GFRP bar was ruptured at failure whereas the steel rebar was buckled, resulting in a larger strain. Nevertheless, both the strains significantly exceeded the expected crushing strain of concrete (ε'_c is typically -0.003 to -0.004 depending on the confinement level).

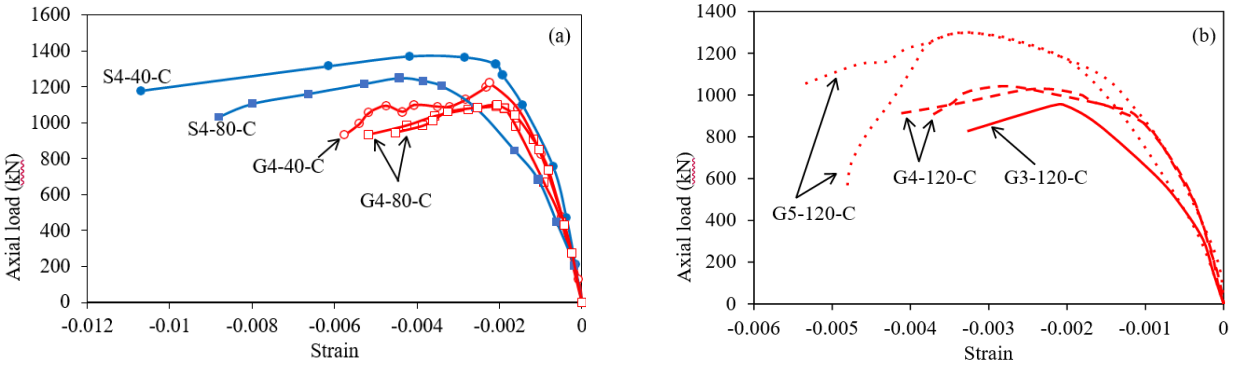

a) steel- and GFRP- reinforced columns with 4 longitudinal bars b) GFRP-reinforced columns with a 120 mm spiral pitch.

Figure 5. Strains developed in the longitudinal bars of concentrically loaded columns.

The Column specimens with 80m pitch (G4-80-C and S4-80-C) exhibited a single peak load with greatly reduced ductility compared with 40mm pitch (G4-40-C and S4-40-C). The results demonstrate that at a larger spiral pitch, the susceptibility to buckling become more critical to the stability of the columns, hence the larger difference in peak load between the steel and GFRP reinforcement. It was observed that after the peak load, a significant drop in axial load was occurred for both columns due to the fact that shear cracks were quickly developed in the concrete specimens. It is obvious that rupturing and buckling occurred in the longitudinal GFRP bars and steel rebars, respectively, and no subsequent peaks were observed.

The results demonstrate that the concrete specimens with insufficient confinement from the spirals, failed in shear in both columns as shown in Figure. 3. It is worth noting that the region where spalling of the cover occurred reduced significantly in size compared to those with a 40 mm pitch. The column collapsed sooner after the onset of cracking due to a more localized plasticity distribution. As shown in Figure 6a, the strain in the steel rebar ($\varepsilon_{s,\,c}$ = -0.010) was higher than that in the GFRP bar ($\varepsilon_{frp,\,c}$ = -0.005). Both values were found smaller than those in specimens with a 40 mm pitch. This demonstrate that high strains can be achieved by adequate transverse confinement.

Figure 5b shows the results of the column specimens with 120mm pitch (G3-120-C, G4-120-C and G5-120-C) produced one single peak and had a substantial reduction in load during the post-peak collapse. The additional longitudinal reinforcement resulted in a more ductile failure mode, which was shown in the transition from a progressive failure with 5 bars to a brittle failure with 3 bars. The three specimen columns had exhibited distinct elastic moduli in the elastic range but varying peak loads, indicating the contribution of the longitudinal GFRP bars to the load capacity of the column in compression. This is likely attributed to the fact that the large number of restrained GFRP long bars act like a shell and thus had a significant effect on the confined concrete contribution towards the load carrying capacity.

The results of Figure 3 and Figure 6 show that increasing the spiral pitch from 40 mm to 120 mm resulted in ductility of the columns is reduced drastically. Additionally, the collapsing process changed from multiple peaks to a single peak with an explosive failure. This signify the importance of having adequate transverse reinforcement to improve the load capacity, obtain the favorable ductile failure mode and reduce the stiffness difference from substituting the steel rebars to GFRP bars.

The columns eventually failed under concentrically loading after a critical number of ruptures in the GFRP spirals, causing buckling or rupturing of the longitudinal bars and crushing of the concrete specimens. Figure 7 shows a typical testing of the concentrically loaded column specimens.

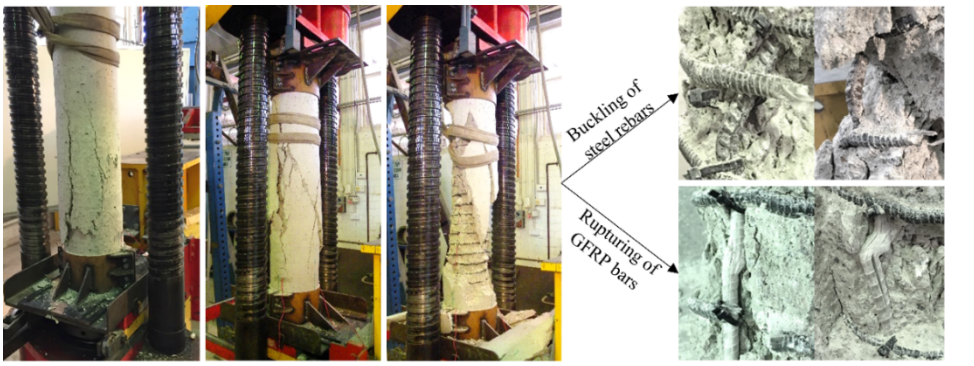

Figure 7. Testing of a concentrically loaded column.

3.1 Eccentrically loaded columns at e=25mm

Figure 8 (a and b) shows the results for eccentrically loaded columns reinforced with 4 longitudinal GFRB bars at a 40 and 80mm spiral pitch respectively. The Column G40-40-25 exhibited a slight stiffer response in the elastic range but a 15% higher load capacity than that of G40-80-25. Although the two column

specimens showed similar post peak responses, the reduction in the load after the peak was 50% higher for G4-80-25 whilst it was about 30% reduction for G4-40-25.

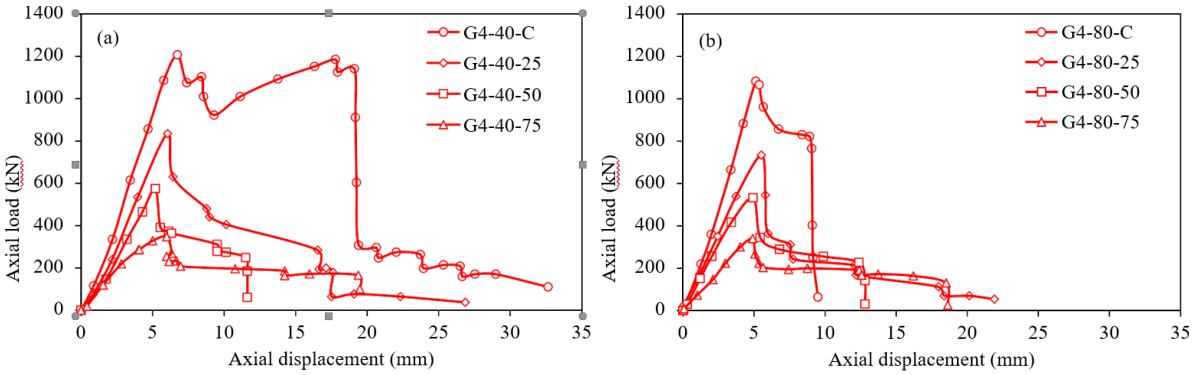

a) 40 mm spiral pitch

b) 80 mm spiral pitch.

Figure 8. Axial load-axial displacement curves of the eccentrically loaded columns.

Figure 9 (a and b) shows the strains developed in the longitudinal bars of the eccentrically loaded columns 40 mm and 80 mm spiral pitch respectively. The results shows that with a higher reinforcement ratio, G4-40-25 was able to sustain a higher deflection. The compressive strain extended to $\varepsilon_{frp,\,c}$ = -0.008 in G4-40-25 and $\varepsilon_{frp,\,c}$ = -0.006 in G4-80-25. At the early stage of loading, the GFRP bars were initially in compression at the tension face due to the low eccentricity then the tensile strains developed after the peak, where significant deflection occurred. The maximum tensile strain recorded were approximately $\varepsilon_{frp,\,t}$ = 0.002 for both columns.

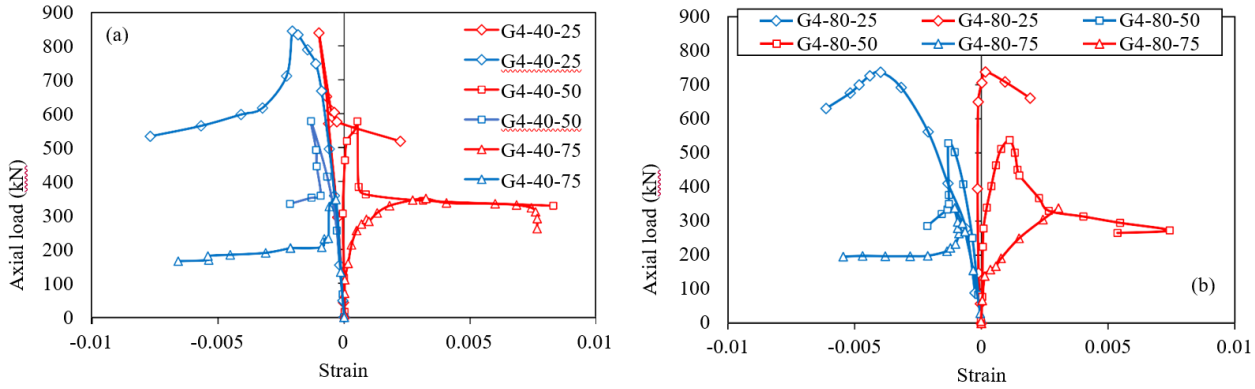

a) 40 mm spiral pitch

b) 80 mm spiral pitch.

Figure 9. Strains developed in the longitudinal bars of the eccentrically loaded columns.

Figure 10. Eccentrically loaded columns after testing.

Figure 10 shows the tensile cracks and the crushing of concrete occurred towards the lower end of column G4-40-25. It showed a uniform distribution of the tensile cracks near the failed region whilst G4-80-25 failed at the mid-height due to the crushing of concrete on the compression face.

3.1 Eccentrically loaded columns at e=50mm

The results in Figure 8 (a and b) shows that the columns G4-40-50 and G4-80-50 both exhibited a similar elastic range but with a reduction in ductility post-peak when compared to their counterpart at e= 25mm. The column G4-40-50 was able to sustain two ruptures in the spirals, while one rupture was only noted to cause the collapse of G40-80-50. The difference in the peak was about 8% between the two columns, smaller than that of columns loaded at e=25mm.

Figure 9 shows that the strains in G4-40-50 reached $\varepsilon_{frp,\,c}$ = -0.002 and $\varepsilon_{frp,\,t}$ = 0.008 whereas the strains in G4-80-50 reached $\varepsilon_{frp,\,c}$ = -0.002 and εfrp, t = 0.007. The results show that as the eccentricity increased, the contribution of the concrete gradually decreased. This is attributed to the contribution of the increasing proportion of the section in tension.

At failure, the tensile GFRP bars in Column G4-80-50 slipped due to insufficient restraint whilst the in G4-40-50 with proper amount of restraint, the GFRP bar reached higher tensile strains without pulling out. Fig 10 shows that the column failed due to the crushing of concrete on the compression faced. This is attributed to the formation of a plastic hinge resulting in high localised bending (Elchalakani et al. 2018a). It appears that some preventative measures in design can be adopted by increasing the number or size of the longitudinal reinforcement.

3.1 Eccentrically loaded columns at e=75mm

Figure 8 shows that the columns G4-40-75 and G4-80-75 both exhibited a similar elastic range and similar post-peak response. The columns G4-40-75 exhibited 2.3% higher load capacity than that of G4-80-75, much lower than those loaded at lower eccentricities due to the well confined effects. At the early stage of loading, the tensile cracks were initially developed quickly on the tension side into a larger crack, splitting the concrete sections into two halves. The failure composed of rupturing of both GFRP bars on the tension face and crushing of concrete on the compression face. The results in Figure 9 show that the compression strains reached $\varepsilon_{frp,\,c}$ = -0.005 to -0.006 until the catastrophic failure occurred on the compression face. Fig ure 10 shows that both columns deflected substantially, rupturing the two GFRP bars in tension and collapsed over a short time, with splitting to two halves at mid height.

3. Conclusions

A total of 13 concrete columns reinforced with GFRP and conventional steel bars were tested and the following conclusions are drawn:

1. A high transverse reinforcement ratio in concrete corresponded to an improved failure mode, increased ductility and enhanced load capacities. By reducing the pitch of GFRP stirrup from 80 mm to 40 mm, the ductility and load capacity increased by 38% and 10% on average.
2. Columns with more longitudinal GFRP reinforcement exhibited higher load capacities and ductility indices. The longitudinal GFRP bars enhanced the confinement effect of the transverse GFRP reinforcement..
3. The difference in load capacities between steel and GFRP-reinforced columns decreased as the amount of transverse reinforcement increased. With the same longitudinal and transverse reinforcement ratio, GFRP-reinforced columns were more ductile than their steel counterparts.
4. The difference in the load capacity of columns with 40 mm and 80 mm spiral pitch decreased from 15.5% at low eccentricity to 2.3% at high eccentricity. The difference in ductility decreased from 40.7%

to 3.0% at the same time. This was attributed to the reducing confining effect of the transverse reinforcement due to eccentricity.

4. Acknowledgement

The authors are grateful for the donations and support provided by Pultron Composites, New Zealand and Anthony Miles from Sika Australia. Appreciation is also given Ms Ella Kepic, laboratory technicians Mr Jim Waters, Mr Brad Rose and Mr Matt Arpin for their help with the many practical aspects of this project.

5. References

1. ACI. (2008). 440.6-08(17) Specification for Carbon and Glass Fiber-Reinforced Polymer Bar Materials for Concrete Reinforcement (Reapproved 2017).
2. ACI. (2015). 440.1R-15 Guide for the Design and Construction of Concrete Reinforced with FRP Bars. American Concrete Institute, Farmington Hills, MI, USA.
3. ACI 318. (2014). Building Code Requirements for Structural Concrete and Commentary. American Concrete Institute.
4. Alsayed, S. H., Almusallam, T. H., Amjad, M. A., and Al-Salloum, Y. A. (1999). “Concrete Columns Reinforced by Glass Fiber Reinforced Polymer Rods.” ACI Special Publication, 188, 103–112.
5. AS/NZS 4671. (2001). Steel reinforcing materials. Standards Australia.
6. AS. (2018). AS 3600: Concrete structures. Standards Australia.
7. AS 1012.11. (2014). AS 1012.11-2000 Methods of testing concrete - Determination of the modulus of rupture. Standards Australia.
8. AS 1012.3.5. (2015). Determination of properties related to the consistency of concrete—Slump flow, T500 and J-ring test. Standards Australia.
9. ASTM C1621-17. (2017). Standard Test Method for Passing Ability of Self-Consolidating Concrete by J-Ring. ASTM International, West Conshohocken, PA.
10. CAN/CSA. (2014). A23.3-14 Design of concrete structures. CSA Group.
11. CAN/CSA. (2017). S806-02 Design and Construction of Building Components with Fibre-Reinforced Polymers. Canadian Standards Association, Ontario.
12. CAN/CSA S6-06. (2006). Canadian Highway Bridge Design Code. Can/Csa-S6-06, Cana, Ontario
13. Desayi, P., and Krishnan, S. (1964). “Equation for the Stress-strain Curve of Concrete.” Journal of the American Concrete Institute, 61(3), 345–350.
14. Elchalakani, M., Dong, M., Karrech, A., Li, G., Mohamed Ali, M. S., and Manalo, A. (2018a). “Behaviour and design of air cured GFRP-reinforced geopolymer concrete square columns.” Magazine of Concrete Research, 1–63.
15. Elchalakani, M., Dong, M., Karrech, A., Li, G., Mohamed Ali, M. S., and Yang, B. (2019). “Experimental Investigation of Rectangular Air-Cured Geopolymer Concrete Columns Reinforced with GFRP Bars and Stirrups.” Journal ofComposites for Construction.
16. Hadhood, A., Mohamed, H. M., and Benmokrane, B. (2016). “Experimental Study of Circular High-Strength Concrete Columns Reinforced with GFRP Bars and Spirals under Concentric and Eccentric Loading.” Journal of Composites for Construction, 3(2014), 04016078.
17. Pultron Composites. (2016). MateenBar – Technical Submittal.